LABORATORI NAZIONALI DI FRASCATI
SIS – Pubblicazioni

LNF-04/03 (IR)
17 Febbaio 2004

PolyCAD: A NEW X-RAY TRACING CODE FOR CYLINDRICAL POLYCAPILLARY OPTICS

D. Hampai[1], S.B. Dabagov[2,3], and G. Cappuccio[1, 2]

[1)] CNR - Istituto per lo Studio dei Materiali Nanostrutturati, 00016 Montelibretti (RM), Italy

[2)] INFN Laboratori Nazionali di Frascati, CP 13, I-00044 Frascati, Italy

[3)] RAS - P.N. Lebedev Physics Institute, 119991 Moscow, Russia

Abstract

A new CAD program designed for X-ray photon tracing in polycapillary optics is described. As starting approach the simplest case of cylindrical polycapillary optics is presented. The *PolyCAD* allows any type of X-ray source such as an X-ray tube of finite beam dimensions as well as an astrophysical object in combination with polycapillary optical samples to be simulated. Using geometrical optics approximation the program was drawn up by a code for two different sources: a point-source and an X-ray tube. The radiation distributions formed by the cylindrical lens on a screen located at various distances are discussed. The agreement with the results earlier published validates the PolyCAD results.

PACS: 07.85.Fv, 41.50.+h, 42.25.-p

1 Introduction

Polycapillary optics, as instrument to manage X-ray and neutron beams, were proposed for the first time by M.A. Kumakhov just in the middle of 1980s [1,2], although possibility for using a single capillary tube (a monocapillary) as a guide of X-ray beams was discovered long time ago [3,4]. Polycapillary optical elements are typically formed by the bundles of glass capillaries (glass can be replaced by other substance in dependence on the purpose for the optics's use, or can be of different compositions), straight or tapered, with many hundred micro-channels. Now, after about 25 years of research and development in polycapillary optics, this new technique provides efficient focusing and bending of X-ray beams, transformation of a divergent beam into a parallel one and vice-versa without strong absorption of radiation. Presently the fifth generation of polycapillary optical elements is let out; they are rather small in sizes (just a few cm in length and a couple of mm in diameter) with many thousands sub-micron channels [5,6].

Nowadays the use of polycapillary lenses to handle X-ray beams is becoming of increasing importance in many analytical apparatuses for X-ray diffraction, X-ray fluorescence, etc. In the nearest future the use of such optics will be surely common in many different fields like aero-space research, medicine, biology, etc. [7]. Strong attraction to the development of such devices pushed the idea to create a CAD program that makes it possible to simulate the process of radiation propagation through polycapillary optical systems in order to calculate the radiation parameters behind the optics. The process of radiation transportation by capillary channels is rather complex, and to describe it needs the solution of precise mathematical equation of radiation propagation that takes into account wave features of scattering inside the guide channel (see, for instance, [8,9]).

Obviously, for the period of more than two decades a number of articles describing ray-tracing algorithms for X-radiation transportation by capillary channels was published [10–13]. Each of them allowed analyzing the propagation process with some specifications, which were defined by the approximation procedures used. By means of these algorithms it became possible to explain interesting features of X-ray transmission by capillary systems.

Here we present a new CAD program that demonstrates how a simple cylindrical polycapillary optics (*CPO*) can deal with different shaped X-ray sources:

- X-ray point-source located at finite distance from the optics, which produces a divergent X-ray beam;

- X-ray source of typical configuration, which can be found in many X-ray apparatuses.

2 Geometry of propagation

To treat the propagation of X-ray photons through the polycapillary channels we will use the ray optics approach, within of which the Snell's law governs reflection of radiation from the surface, because, in the first approximation, we can neglect the wave features of radiation propagation.

Let us introduce the geometry of X-ray travel inside the capillary systems, neglecting the absorption and/or diffusion effects. Due to the symmetry of system geometry, the reflection angle α_{ref}, in Fig. 1 and Fig. 2, remains constant for each possible interaction with the channel surface. For each photon three physical parameters are included in the mathematical treatment: I) the incidence angle α; II) the intersection point $P_0(x_0, y_0)$ of the photon trajectory with the inlet plane (I_p); and III) the photon energy, which is related to the maximum allowed incident angle that, in optimal case, is the so-called *critical angle of total external reflection* or *Fresnel angle* θ_c. If the surface is made by glass the critical angle can be evaluated by:

$$\theta_c\,[mrad] \simeq \frac{30}{E\,[keV]} \tag{1}$$

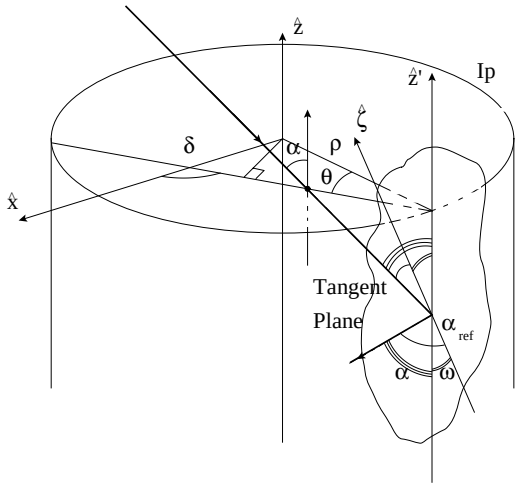

Figure 1: Three dimensional draw of photon reflection from the capillary wall. The photon path is shown by the bold line. I_p is the transverse cross section plane at the capillary entrance. Details of the interaction zone are shown in Fig. 2.

The reflection angle α_{ref} is given by the following formula:

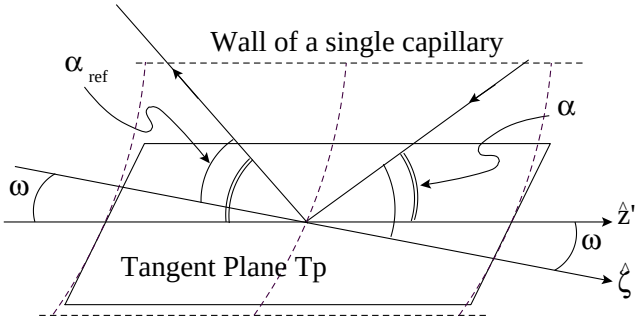

Figure 2: The angles α, ω and α_{ref} that the photon trajectory forms with respect to the $\hat{z}'$- and $\hat{\zeta}$-axes are shown. The $\hat{z}'$-axis is parallel to the $\hat{z}$-axis, while the $\hat{\zeta}$-axis is a projection of the photon path onto the tangent plane T_p.

$$\alpha_{ref} \;=\; \arccos\left(\frac{\cos\alpha}{\cos\omega}\right)\,, \tag{2}$$

where α is the *incident angle*, while the *axial angle* ω is formed by the projection of photon path onto the tangent plane (T_p) and the line $\hat{z}'$, which is parallel to the $\hat{z}$ axis. The ω angle is specified by two parameters: the incident angle α and the θ angle. The last is defined by the capillary radius ρ and the projection of photon path onto the inlet plane (I_p) (look at Fig. 1). Taking into account the expression

$$\omega \;=\; \arctan\,\left(\tan\alpha\cdot\sin\theta\right), \tag{3}$$

Eq.(2) can be written in the form

$$\alpha_{ref} \;=\; \arccos\left\{\frac{\cos\alpha}{\cos\left[\arctan\,\left(\tan\alpha\cdot\sin\theta\right)\right]}\right\}. \tag{4}$$

Now we would like to emphasize that due to the cylindrical symmetry of geometry considered, for each incident photon that enters a capillary channel, the angle of reflection α_{ref} remains unchanged during the propagation. As photons propagate in *total external reflection regime*, the amplitude of reflection can be taken as constant because of the fact that there is no any energy dispersion. As a consequence for each trajectory path the heights h of the projections to the $\hat{z}'$-axis between two successive reflections remain the same and are given by the relation

$$h \;=\; 2\,R\,\cos\theta\,\cot\alpha \tag{5}$$

For the first and the last steps the heights must be evaluated separately.

3 Algorithm description

Following the geometry of scattering above presented, a special algorithm for simulating radiation propagation through capillary systems was elaborated in the FORTRAN computer language.

The FORTRAN code is divided in three main parts. In the first, the main physical and geometrical parameters of optical system are determined, namely, the type of capillary (mono- or polycapillary) to be studied.

In the second part, for each photon, the initial conditions, i.e. the α angle and the intersection point P_0, are defined by means of a random routine that is correlated with one of the above mentioned photon sources as a point (mathematical) source located at infinite distance or as a limited (physical) source located at finite distance.

The last section is the core of the code: at the beginning of the subroutine the main parameters α_{ref} and h, are evaluated by Eqs.(4) and (5); then a loop of successful calculations in dependence on a number of photon interactions with capillary wall is done. The exit file collects all the evaluated data.

4 Results and discussion

First of all, in order to check all the software procedures we have considered the following conditions: 1) a 1 keV source with infinite extension located somewhere in the space; 2) all X-ray photons will have the same incidence angle α; 3) photons enter a cylindrical monocapillary of 10 cm length and $\rho = 10^{-3}$ cm radius. Each photon has random direction, i.e. its projection onto the (xy) plane forms a random angle, δ.

Each point in Fig. 3 corresponds to the photon coordinate in the inlet plane that has success in passing through the capillary in a completely random way.

Fig. 4 represents the image collected on a screen at distance of 10 cm from the exit. It is evident that the points' density is higher at the edge of the picture. It happens due to the fact that main portion of the beam propagates through a capillary near the channel surface by multiple reflection mechanism, and a number of photons undergoes just a few reflections, is rather small.

Now instead of an infinite source, in Fig. 5 we will consider a point-source. All other parameters will remain the same, however, with two specific conditions: 1) the distance from the source to the inlet plane is given by the condition to have no more than three reflections, and 2) the inlet angle δ is given by the formula

$$\delta = \arctan\left(\frac{y_0 - y_s}{x_0 - x_s}\right), \tag{6}$$

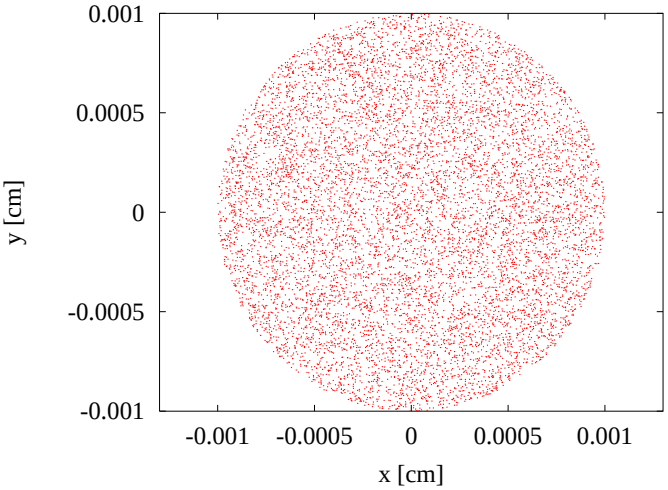

Figure 3: This picture represents the inlet plane of a monocapillary for every successful photon crossing. Each point is the coordinate where the photon enters. It is evident that all the area is homogeneously filled by random events. The parameters are a source of infinite extension with 1 keV energy, while the monocapillary has 10 cm in length and a radius of 10 μm.

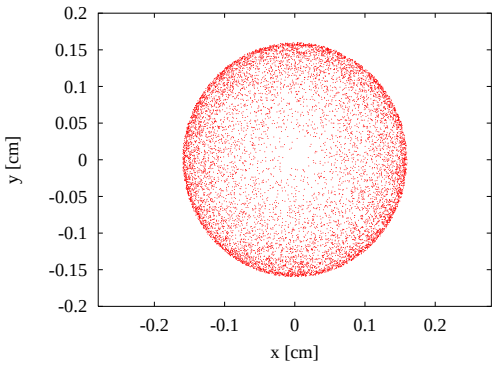

Figure 4: The output image collected on a screen in case of fixed incident angle for a single capillary. This picture is taken at the exit of the case described in the fig.3 with a distance from the capillary to the screen of 10 cm.The density is higher at the edge of the guide.

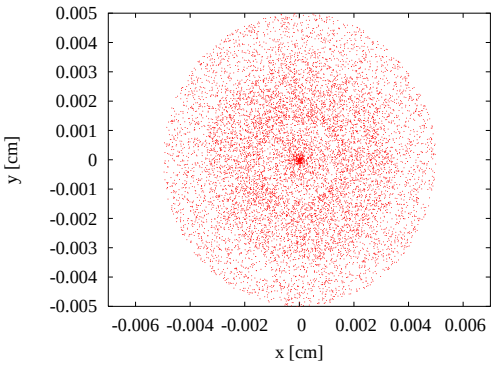

Figure 5: The output image for a monocapillary detected on a screen in case of a point-source. To compare with figures 3 and 4, simulations were performed with the same geometrical parameters.

where $(x_s,\, y_s)$ is the source coordinate in the (xy) plane: we take the simplest case, where x_s and y_s are equal to zero.

It is also interesting to study a point-source at finite distance so that the incident angle α can be chosen in a random way from zero to any fixed angle. Obviously, in optimal case this angle is equal to the critical one, $\alpha = \theta_c$. Moreover, each X-ray photon will have an inlet angle δ in the I_p plane that is strictly connected with an intersection point $P_0\,(x_0,\, y_0)$ by the formula (6).

To simplify analysis of the radiation distributions behind a capillary system, we have considered the following image shapes in four different screen positions (Cf. Fig. 6). The screen is placed at the exit of monocapillary or polycapillary (1), the distance between the capillary and the screen is equal to the distance between the source and the capillary (f), while (2) is an intermediate position between (1) and (f), and finally the screen position (3) is beyond the (f) position.

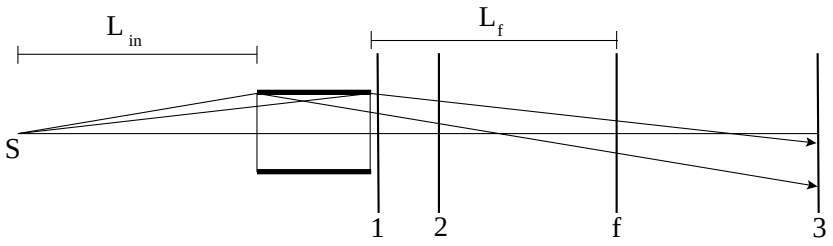

Figure 6: Geometry of the computer experiment for four different screen positions: (1), (2), (f), and (3).

Here we will present only the images formed by a monocapillary and by a polycapillary, with the same geometrical parameters and the same number of X-ray photons, in the (f) position when the distance L_{in} is equal to L_{out}. In order to compare our calculations with the results previously obtained [14], we have chosen the length of monocapillary that provides a single reflection mode of propagation. The final results are visualized in Figs. 7, 8 and 9. In Fig. 7 there is a single spot and an halo of uniform density distribution by straight fly-by (without reflection) rays, while in Fig. 8 there are three rings: the inner end the medium ones are due to the one and two reflections, while the origin of external ring is due to the halo. For polycapillary case (Fig. 9) one can observe a slight bigger spot while the point density distribution of the halo is decreasing going from the center to the periphery.

The power of PolyCAD program is that it can deal with any geometrical and optical configuration. It means that we may easily simulate the behaviour of a source of finite

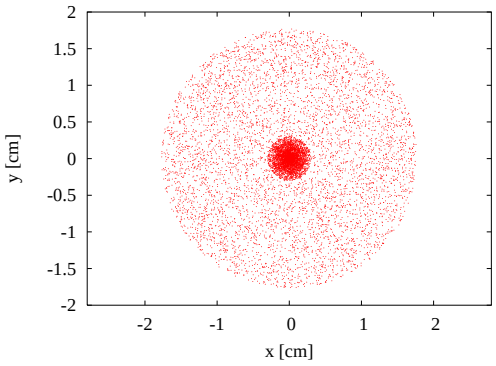

Figure 7: The image on a screen behind a monocapillary in the case of a point-source. The central intense spot is formed by photons reflected from the inner capillary surface, while the halo is due to photons that pass without interactions. The parameters are: 1 cm radius, 1 keV energy, and $L_{in} = L_{out} = 33$ cm.

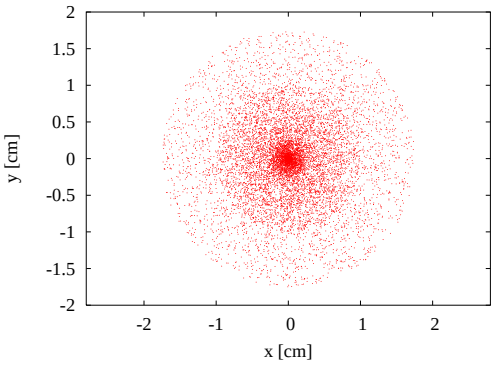

Figure 8: The output image for a monocapillary obtained on a screen in case of a point-source. The length of the capillary has been chosen to show three different rings, formed by one and two reflection modes; the external halo is due to photons that pass without interactions.

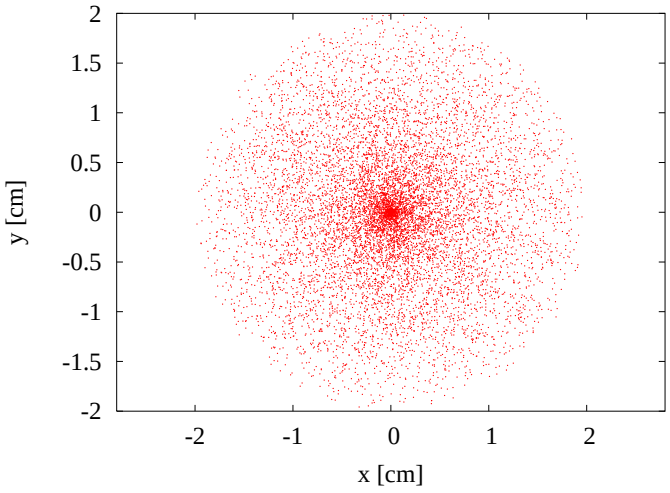

Figure 9: The image of a point-source on a screen behind a polycapillary. Here one appears an intense central spot of a diameter slight bigger than in case of monocapillary. The main difference is that here the halo is not homogeneous, and it disappears at the edge of the picture. The parameters are as above while the radius of the polycapillary is 1 cm and the radius of each capillary is 10^{-3} cm.

dimensions like, for example, conventional X-ray tube. In order to treat this situation an offset for a single point-source is introduced in the program. In such a mode a finite area source can be simulated by random distribution of points inside a specific area. As practical application let to consider a 'Long Fine Focus' of X-ray tube (for instance, a Cu anode, 8 keV), where the electron spot on the anticathode has the dimension of 0.4×12 mm. Such kind of tube allows us to have both an 'optical point-focus' (Fig. 10) and an 'optical line-focus' (Fig. 11). The source dimensions are respectively 0.4×1.2 mm and 0.04×12 mm.

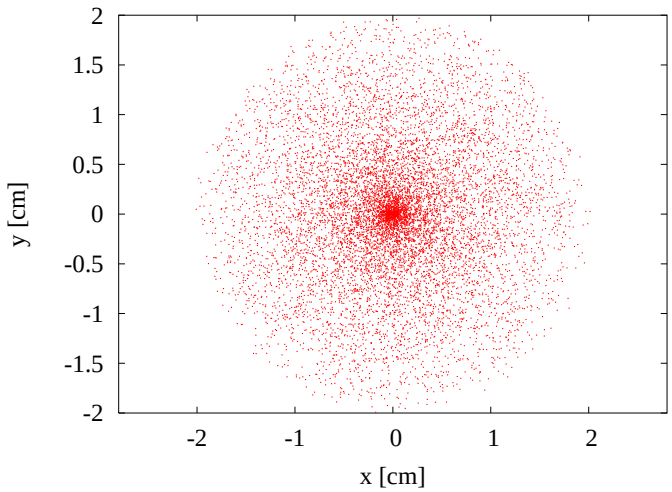

Figure 10: The image formed on the screen by the cylindrical polycapillary, when the 'optical point focus' of a Cu tube has been used.

Analyzing Figs. 10 and 11 we can resolve different shapes of the central spot area, according to the shapes of two 'optical focuses' used in simulations. Moreover, in Fig. 11 the halo shows a quasi-elliptical trend due to the 'optical line focus' used.

5 Conclusion

In this work we have first reported a new CAD program designed for capillary optics. The algorithm allows the travel of X-ray beam inside the polycapillary channels for the sources of different shapes to be simulated using ray optics approximation in the ideal case without absorption, as well as the spot images formed on a screen at different distances from the optics to be visualized.

After description of the computational details, the numerical analysis is given for various configurations. In case of a cylindrical monocapillary we found a good agreement

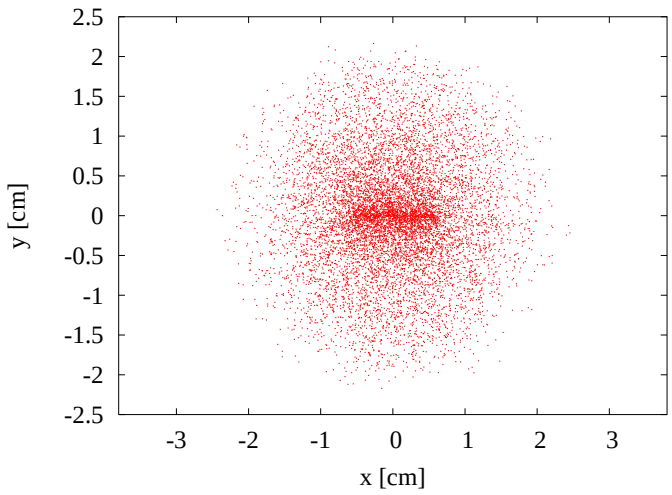

Figure 11: The image behind cylindrical polycapillary sample when the 'optical line focus' of a Cu tube has been used.

with the results for various cases of single and multiple reflection modes that have been previously discussed [11,14]. In the following publications we are going to present the work, which at present in progress, to increase the CAD program abilities for treating other shapes of polycapillary optics like conical, semi-lens and full-lens ones. However, for understanding the fine features of X-ray propagation through the polycapillary lenses it is mandatory to consider X-ray wave interaction with inner capillary surface (details in the review [15]), and this will be the future development of the *PolyCAD* program.

6 Acknowledgments

We are grateful to M.A. Kumakhov for his continuous interest and support, and G. Cibin for fruitful suggestions in the development of the FORTRAN code. This work was done within the frame of the FISR Project 'Multipurpose Innovative Plants for the UV and X-ray Production', CNR - MIUR (2003-2005), and was partly supported by the POLYX project (Group V, LNF - INFN).

References

[1] M. A. Kumakhov, *Patent 1322888*, 1984.

[2] M. A. Kumakhov and F. F. Komarov, *Phys. Rep.*, Vol. **191(5)**, 289-350, 1990.

[3] P.B. Hirsch, and J. Kellar, *Proc. Phys. Soc. London Scr.*, Vol. **B64**, 369, 1951.

[4] E. Pound, and C. Rebka, *Phys. Rev. Lett.*, Vol. **3**, 439, 1959.

[5] M. A. Kumakhov, *Proceedings SPIE*, Vol. **4155**, 2-12, 2000

[6] http://www.unisantis.com, or http://www.iroptic.com

[7] V.V A.A, in 'Selected Papers on Kumakhov Optics and Application 1998-2000', Part II, 'Application of capillary optics', *Proceedings SPIE*, Vol. **4155**, 100-150, 2000.

[8] G. Cappuccio, S.B. Dabagov, A. Pifferi, and C. Gramaccioni, *Appl. Phys. Lett.*, Vol.**78(19)**,2822-2824, 2001.

[9] S.B. Dabagov, A. Marcelli, G. Cappuccio, and E. Burattini, *Nucl. Instr. Meth.*, Vol.**B187 (2)**, 169-177, 2002.

[10] K.Furuta, Y. Nakayama, M. Shoji, et al., *Rev. Sci. Instr.*, Vol. **64**, 135, 1993.

[11] L. Vincze, K. Janssens, F. Adams, and A. Rindby, *X-Ray Spectrom.*, Vol.**24**, 27, 1995.

[12] D.J. Tiel, *J. Synchrotron Rad.*, Vol. **5**, 820, 1998.

[13] Chen Baozhen, *Nucl. Instr. Meth.*, Vol. **B170**, 230, 2000.

[14] S.B. Dabagov, and A. Marcelli, *Proc. of SPIE*, Vol. **4155**, 92, 2000; *Appl. Opt.*, Vol.**38(36)**, 7494-7497, 1999.

[15] S.B. Dabagov, *Physics Uspekhi*, Vol.**46(10)**, 1053-1075, 2003.